Radiology: Cardiothoracic Imaging

ORIGINAL RESEARCH

Molecular Imaging of Diffuse Cardiac Fibrosis with a Radiotracer That Targets Proteolyzed Collagen IV

*Be'eri Niego, PhD** • *Bianca Jupp, PhD** • *Nicholas A. Zia, MSc* • *Rong Xu, PhD* • *Edwina Jap, BSc* • *Martin Ezeani, PhD* • *Asif Noor, PhD* • *Paul S. Donnelly, PhD* • *Christoph E. Hagemeyer, PhD*** • *Karen Alt, PhD***

From the NanoBiotechnology Laboratory (B.N., R.X., M.E., C.E.H.) and NanoTheranostics Laboratory (E.J., K.A.), Australian Centre for Blood Diseases, Central Clinical School, Monash University, Melbourne, VIC 3004, Australia; Department of Neuroscience, Central Clinical School, Monash University, Melbourne, Australia (B.J.); and School of Chemistry and Bio21 Molecular Science and Biotechnology Institute, University of Melbourne, Melbourne, Australia (N.A.Z., A.N., P.S.D.). Received April 5, 2023; revision requested June 2; revision received November 19; accepted January 22, 2024. **Address correspondence to** K.A. (email: *karen.alt@monash.edu*).

Supported by grant awarded to C.E.H. by the National Health and Medical Research Council of Australia (NHMRC) (grant no. GNT1120129) and by a Vanguard Grant (grant no. 106859) awarded to B.N., K.A., and C.E.H. by the Heart Foundation of Australia. M.E. is supported by a Government of Australia Training Research Program Scholarship and the Monash University, Faculty of Medicine, Nursing and Health Sciences Postgraduate Excellence Award. K.A. is an NHMRC Medical Research Future Fund Career Development Fellow (award no. GNT1140465). C.E.H. is a senior research fellow of the NHMRC of Australia (award no. GNT1154270). B.N. is supported by a Vanguard Grant (grant no.106859) from the Heart Foundation of Australia and by an NHMRC grant (grant no. GNT1120129). P.S.D. was supported by the Australian Research Council and the NHMRC (award no. 2011853).

*B.N. and B.J. contributed equally to this work.

**C.E.H. and K.A. are co–senior authors.

Conflicts of interest are listed at the end of this article.

Radiology: Cardiothoracic Imaging 2024; 6(2):e230098 • https://doi.org/10.1148/ryct.230098 • Content codes: CA MI

Purpose: To develop an approach for in vivo detection of interstitial cardiac fibrosis using PET with a peptide tracer targeting proteolyzed collagen IV (T-peptide).

Materials and Methods: T-peptide was conjugated to the copper chelator MeCOSar (chemical name, 5-(8-methyl-3,6,10,13,16,19-hexaazabicyclo[6.6.6]icosan-1-ylamino)-5-oxopentanoic acid) and radiolabeled with copper 64 (^{64}Cu). PET/CT scans were acquired following intravenous delivery of ^{64}Cu-T-peptide-MeCOSar (0.25 mg/kg; 18 MBq ± 2.7 [SD]) to male transgenic mice overexpressing β2-adrenergic receptors with intermediate (7 months of age; n = 4 per group) to severe (10 months of age; n = 11 per group) cardiac fibrosis and their wild-type controls. PET scans were also performed following coadministration of the radiolabeled probe with nonlabeled T-peptide in excess to confirm binding specificity. PET data were analyzed by t tests for static scans and analysis of variance tests (one- or two-way) for dynamic scans.

Results: PET/CT scans revealed significantly elevated (2.24–4.26-fold; $P < .05$) ^{64}Cu-T-peptide-MeCOSar binding in the fibrotic hearts of aged transgenic β2-adrenergic receptor mice across the entire 45-minute acquisition period compared with healthy controls. The cardiac tracer accumulation and presence of diffuse cardiac fibrosis in older animals were confirmed by gamma counting ($P < .05$) and histologic evaluation, respectively. Coadministration of a nonradiolabeled probe in excess abolished the elevated radiotracer binding in the aged transgenic hearts. Importantly, PET tracer accumulation was also detected in younger (7 months of age) transgenic mice with intermediate cardiac fibrosis, although this was only apparent from 20 minutes following injection (1.6–2.2-fold binding increase; $P < .05$).

Conclusion: The T-peptide PET tracer targeting proteolyzed collagen IV provided a sensitive and specific approach of detecting diffuse cardiac fibrosis at varying degrees of severity in a transgenic mouse model.

Diffuse cardiac fibrosis is a key pathologic process accompanying many cardiovascular diseases in which excess extracellular collagen builds up in the heart muscle and weakens its function. Several collagen types and collagen-modifying enzymes were shown to be upregulated in the human heart during cardiovascular diseases including the structural type I collagen, the basement membrane type IV collagen (1), and matrix metalloproteinases (MMPs) (2). Cardiac collagens and their digested forms thus become excellent targets for direction of imaging agents and/or therapeutics into the diseased heart. Despite this opportunity, medical imaging of diffuse cardiac fibrosis remains an unmet clinical challenge in urgent need of new and innovative solutions. While late gadolinium enhancement at cardiac MRI and T1 mapping of the myocardial wall enable detection of fibrotic patches and indirect demonstration of interstitial fibrosis due to interstitial expansion (3), no sensitive and quantitative imaging methods exist to directly visualize excess interstitial buildup of myocardial collagens.

Recently, we developed a molecular peptide probe, termed *T-peptide*, capable of detecting interstitial collagen deposits in fibrotic mouse hearts (4,5). This tracer selectively binds to MMP-2–degraded collagen IV in both mice and humans (4–6) with pharmacokinetic, biodistribution, and toxicity profiles suitable for in vivo imaging (ie, a short half-life of 9 minutes, negligible accumulation in healthy organs and in the brain, and no obvious toxicity in clearance organs [liver and kidney] [4]). Conceptually, the use of a tracer targeting digested collagen represents a unique way to approach fibrosis imaging from a more sophisticated angle using a smart probe design. While previous peptide-based strategies have targeted extracellular matrix collagens in their intact form (7,8), enzymatically digested collagen

Abbreviations

β2-AR = β2-adrenergic receptor, HF = heart failure, HPLC = high-performance liquid chromatography, MMP = matrix metalloproteinase, Tg = transgenic, Wt = wild type

Summary

A PET tracer targeting proteolyzed collagen IV provided a sensitive and specific method for detection of diffuse cardiac fibrosis at various disease stages in vivo.

Key Points

- An approach that used a collagen IV–targeted PET radiotracer, termed *T-peptide*, was capable of detecting diffuse cardiac fibrosis in the β2-adrenergic receptor–overexpressing transgenic mouse model of heart failure at various disease stages, from intermediate to severe (at 7 to 10 months of age).
- The T-peptide tracer displayed an optimal time-window for PET imaging between 30 and 45 minutes following administration as well as rapid clearance (~9-minute half-life), low toxicity, and affinity toward human collagen IV, making it well-suited for clinical translation.
- This technique may represent a breakthrough in medical imaging of diffuse cardiac fibrosis and possibly various other fibrotic conditions in which collagen IV plays a role.

Keywords

Diffuse Cardiac Fibrosis, Molecular Peptide Probe, Molecular Imaging, PET/CT

uniquely marks active cardiac disease as it is generated by potent MMPs that are upregulated during acute cardiac pathology. Hence, a T-peptide–based strategy could provide a much needed diagnostic tool for diffuse heart fibrosis that also enables patient stratification based on the nature of the individual disease and its potential to progress. These capabilities are not currently possible using standard collagen imaging approaches.

While our earlier work demonstrated the capacity of this T-peptide approach to detect cardiac fibrosis (4), the clinical compatibility of this innovative methodology remained undetermined since the hearts were scanned ex vivo following administration of a fluorescently labeled T-peptide. In vivo assessment of the T-peptide using a clinically relevant imaging modality is therefore essential for its continued development. In the current work, we demonstrate use of the T-peptide, conjugated to the MeCOSar (chemical name, 5-(8-methyl-3,6,10,13,16,19-hexaaza-bicyclo[6.6.6]icosan-1-ylamino)-5-oxopentanoic acid) ligand that forms stable complexes with copper 64 (^{64}Cu) (9) to detect in vivo diffuse cardiac fibrosis in transgenic (Tg) mice overexpressing β2-adrenergic receptors (AR) with PET.

Materials and Methods

Animal Model

Animal experimentation was approved by the Alfred Research Alliance Animal Ethics Committee at Monash University (approval no. E/1941/2019/M). The study used heterozygote male β2-AR Tg mice (10–12) and littermate nontransgenic male controls (wild type [Wt]) at either 9–10.5 months of age (Tg: n = 11; 33–37 g vs Wt: n = 11; 37–44 g) or 6.5–7.5 months of age (Tg: n = 4; 34–46 g vs Wt: n = 4; 33–42 g). Animals were bred by the Precinct Animal Centre of the Alfred Research Alliance and housed in a temperature- and humidity-controlled facility on a 12-hour light-dark cycle with ad libitum access to standard chow (Mice Maintenance Cube; Barastoc) and water. The well-characterized β2-AR mouse model produces a classic age-dependent phenotype of heart failure (HF) (from ~3 months of age) that includes fibrosis and dilated cardiomyopathy (10–12). Furthermore, as we showed that collagen IV and MMP-2 were strongly upregulated in these fibrotic hearts (4), the β2-AR model not only represents a clinically relevant paradigm of progressive HF but is also ideal for assessment of the collagen IV–targeted T-peptide probe. Two aged animals in each group were excluded from the analysis of the static scans due to an unsuccessful intravenous peptide injection based on low bladder accumulation 45 minutes following injection.

T-peptide Synthesis and Preparation for PET Imaging

The T-peptide was synthesized using standard solid phase peptide synthesis as described previously (4). MeCOSar-*N*-Hydroxysuccinimide was prepared according to reported procedures (13) and then added to a mixture of 9-fluorenylmethyloxycarbonyl (Fmoc)-T-peptide in dimethylformamide. The pH of the reaction mixture was adjusted to a pH of 9 by adding $NaHCO_3$, and the mixture was left to react overnight at 45°C. The reaction progress was monitored by electrospray ionization mass spectrometry. Upon completion, the solvent was removed under vacuum and the residue was purified by reverse-phase high-performance liquid chromatography (HPLC) to produce T-peptide-MeCOSar in 48% yield. T-peptide-MeCOSar (Fig 1A, 1B) was then incubated with the radioisotope ^{64}Cu at a 1:2 ratio (peptide [μg]:^{64}Cu [MBq]) for 20 minutes at room temperature then used without further purification (Fig 1B). Radio-HPLC analysis, described below, indicated a high radiochemical purity of 91% and decay-corrected crude radiochemical yield of 91%, resulting in crude product-specific activity of 1.7 MBq/μg. This study confirmed that very low levels of free ^{64}Cu were present following the labeling reaction (Fig 1C).

Radio-HPLC

Radio-HPLC was performed on a Shimadzu ultra-performance liquid chromatography system (Shimadzu) combined with a PET/SPECT radio-thin-layer chromatography scanner and radio-HPLC detector as well as a dual scan-RAM system (LabLogic Systems). A HALO C18 160 Å 150 × 4.6 mm column (Shimadzu) was employed. The mobile phases consisted of 0.1% trifluoroacetic acid in H_2O (buffer A) and 0.1% trifluoroacetic acid in acetonitrile (buffer B). A linear gradient of 100% solvent A to 100% solvent B over 25 minutes at 1 mL/min flow rate was employed (wavelength, 280 nm with UV-VIS detector). The radio-chromatography data of ^{64}Cu-radiolabeled T-peptide was collected and analyzed by Laura software (version 6.0.5.101 SP1; LabLogic Systems).

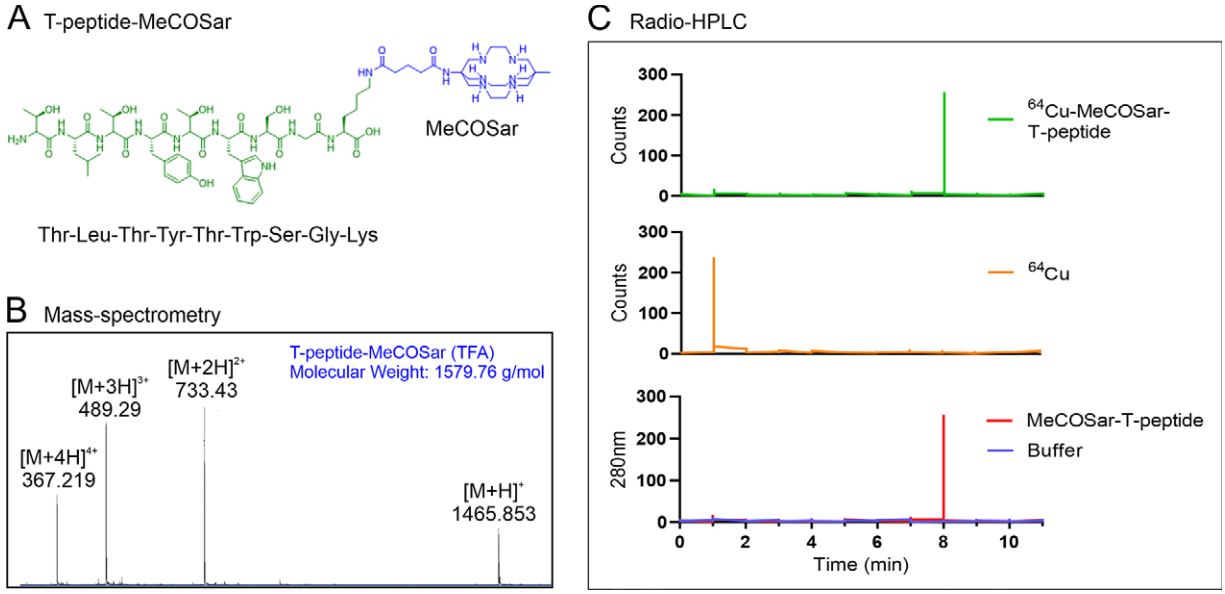

Figure 1: Structure and labeling of copper 64 (^{64}Cu)-T-peptide-MeCOSar (chemical name, 5-(8-methyl-3,6,10,13,16,19-hexaaza-bicyclo[6.6.6] icosan-1-ylamino)-5-oxopentanoic acid). **(A)** The figure shows the chemical structure (peptide sequence in green and the MeCOSar conjugate in blue) and **(B)** mass spectrometry profile of the T-peptide-MeCOSar probe (note that the molecular weight includes trifluoroacetic acid [TFA]). **(C)** Radio–high-performance liquid chromatography (HPLC) chromatogram shows the unlabeled T-peptide-MeCOSar probe (bottom), a free ^{64}Cu radioisotope (middle), and the ^{64}Cu-T-peptide-MeCOSar probe (top) following incubation of peptide and radioisotope at a 1:2 ratio (T-peptide-MeCOSar [μg]:^{64}Cu [MBq]) for 20 minutes at room temperature. No free ^{64}Cu remains following the labeling reaction. Gly = glycine, Leu = leucine, Lys = lysine, Ser = serine, Thr = threonine, Tyr = tyrosine.

In Vivo PET Imaging

^{64}Cu-T-peptide-MeCOSar was intravenously administered into the mouse tail vein at a dose of 10 μg of protein per animal (~0.25 mg/kg; 18 MBq ± 2.7 [SD]). This dose was based on earlier work which used 0.5 mg/kg of fluorescently labeled T-peptide to effectively depict fibrosis by ex vivo scanning in similar animals (4).

Static PET Scans

Thirty minutes following injection, 10.5-month-old mice (Tg: n = 5; Wt: n = 5) were anesthetized by isoflurane (4% induction and 1.5%–2% maintenance in 0.8 L/min oxygen) and placed in a nanoScan PET/CT system (Mediso). PET images were subsequently acquired in list mode for 15 minutes followed by a 10-minute CT acquisition (acquisition parameters: x-ray voltage, 35 kVp [680 μA]; exposure time, 300 msec; and a pitch of 1.0). Over 360° of rotation, 720 projections were acquired with data binning at a 1:1 ratio and then reconstructed using a filtered back-projection algorithm with a Butterworth filter (voxel size, 0.34 μm^3). PET scans were reconstructed into a single static image (voxel size, 0.6 mm^3; matrix size, 80 × 60 × 75 voxels) using the Tera-Tomo three-dimensional algorithm provided by the supplier, with correction for scatter, attenuation, and dead time, and calibrated in kilobecquerel per milliliter.

Dynamic PET Scans

Mice at 9 months of age (Tg: n = 6; Wt: n = 6) or 7 months of age (Tg: n = 4; Wt: n = 4) were anesthetized as described above, and the tracer was injected in a bolus over 10 seconds via the tail vein. A subgroup of three of the 9-month-old Tg mice received a coinjection of 10-fold nonradioactive ("cold") T-peptide (100 μg of protein) together with the radioactive ^{64}Cu-T-peptide-MeCOSar conjugate. Immediately following tracer injection, PET images were acquired for 45 minutes in list mode and reconstructed as described above across the following time frames: 2 × 30 seconds, 3 × 60 seconds, 8 × 300 seconds. Volumes of interest incorporating the heart, kidneys, bladder, and brain were manually delineated on the CT images to extract activity measures from both the dynamic and static PET scans in PMOD (PMOD Technologies).

Postscan Analysis: Gamma Counting and Histology

Following animal euthanasia, the hearts were perfused, collected, and wet weighed and then placed in a gamma counter (Hidex AMG) to calculate the percentage of the initial dose administered per gram of tissue. Hearts were then fixed in formalin, embedded in paraffin, and sliced at 4-μm thick for histologic analysis using Masson trichrome staining. Reactive interstitial fibrosis was imaged by the Aperio AT Turbo digital whole slide scanning system at 20× magnification (Leica Microsystems) and visualized with Aperio ImageScope software (Leica Microsystems). Images were qualitatively assessed for fibrosis by an experienced researcher with over 20 years of cardiovascular research experience (B.N.) who was blinded to the genotype (please note that the quantification of cardiac fibrosis in this model was extensively described by our group [4] and others [12,14]).

Statistical Analysis

Statistical analyses were performed using GraphPad Prism (version 9; GraphPad Software). Data sets were tested for normality by the Shapiro-Wilk normality test and presented as means ± SDs or standard error of the means as specified in the figure legends. Pair-

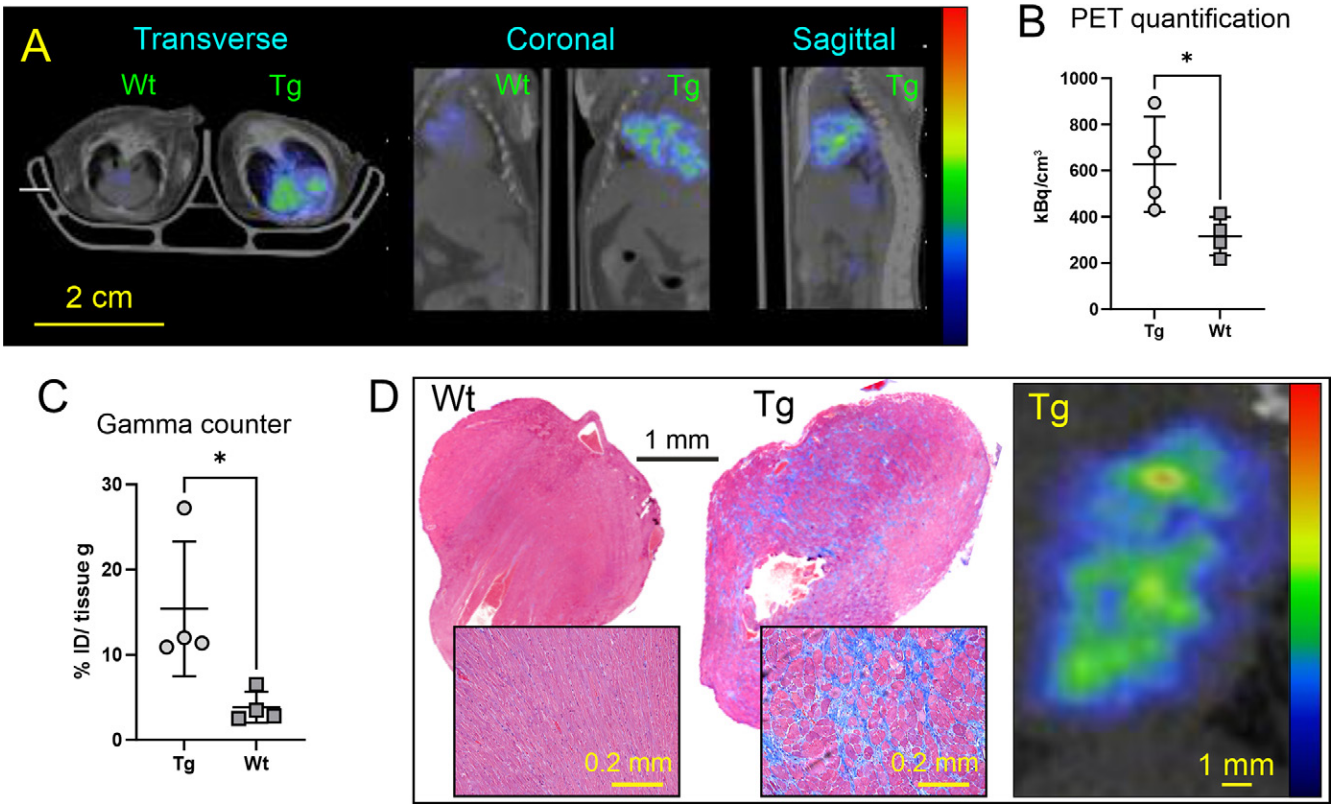

Figure 2: Fibrotic mouse hearts labeled with copper 64 (^{64}Cu)-T-peptide-MeCOSar (chemical name, 5-(8-methyl-3,6,10,13,16,19-hexaaza-bicyclo[6.6.6]icosan-1-ylamino)-5-oxopentanoic acid) at PET. **(A)** Representative PET/CT images (left transverse, coronal, and sagittal) and **(B)** image quantification (in kBq/cm^3) of fibrotic hearts in aged (10–10.5-month-old) transgenic β2 adrenergic receptor–overexpressing mice (Tg) compared with healthy nontransgenic littermate controls (Wt) following intravenous injection of ^{64}Cu-T-peptide-MeCOSar (0.25 mg/kg;18 MBq ± 2.7 [SD]). Images and analysis were generated from data acquired at 30–45 minutes after tracer administration. **(C)** Ex vivo gamma-counter analysis (by percentage of the initial dose [ID] per gram of tissue) confirms a significant uptake of ^{64}Cu-T-peptide-MeCOSar per gram of tissue in Tg versus Wt hearts. **(D)** Similar cardiac distribution patterns of interstitial collagen deposits (blue on a Masson trichrome–stained coronal slice; middle) and ^{64}Cu-T-peptide-MeCOSar radioactivity on a corresponding coronal PET image of the heart (right) support the collagen-binding properties of the T-peptide probe. A healthy coronal heart slice from a Wt mouse is shown on the left. There was a sample size of four per group. Data are expressed as means ± SDs. Scale bars sizes are as specified. Color scale represents PET radiotracer uptake with red corresponding to the highest activity and blue to the lowest activity. * = statistical significance ($P < .05$) by two-tailed Student *t* test.

wise analyses employed a two-tailed Student *t* test. Comparison of three groups or more was done by one-way analysis of variance with Tukey post hoc tests. Comparisons of dynamic PET data over time were performed by two-way repeated-measures one-way analysis of variance (to examine the main effect of time, genotype, and their interaction on tracer uptake). Differences in specific time points were then discerned by post hoc analysis that was either corrected for multiple comparisons by controlling for the false discovery rate with the method of Benjamini, Krieger, and Yekutieli, or analyzed using an uncorrected Fisher least significant difference test (as seen in figure legends). A *P* value less than .05, or a false discovery rate adjusted *P* value (or *q* value) less than or equal to .05, was considered to indicate a statistically significant difference.

Results

PET Imaging with ^{64}Cu-T-peptide-MeCOSar Helps Detect Elevated Tracer Binding in the Fibrotic Mouse Heart

Following preliminary scans to determine the optimal time for static imaging (not shown; see also Kinetics and Specificity of T-peptide-MeCOSar Binding to Fibrotic Hearts below), PET images were acquired between 30 and 45 minutes following radiotracer injection to aged (9–10.5 months old) β2-AR mice. This imaging strategy allowed sufficient time for the tracer (which has a half-life of ~9 minutes [4]) to clear from the blood pool and accumulate at the target. Noticeably, robust retention of the tracer was observed in fibrotic β2-AR Tg hearts compared with minimal tracer accumulation in the healthy controls (Fig 2A). Quantification of the PET imaging data showed a significant increase in tracer uptake in diseased hearts 45 minutes following injection (Wt: 316.4 kBq/cm^3 ± 82.85 vs Tg: 627.3 kBq/cm^3 ± 206.4; $P = .03$; Fig 2B). These results were supported ex vivo by gamma counting–mediated cardiac biodistribution analysis revealing a significant increase in heart tissue uptake (Wt: 3.84 ± 1.83 vs Tg: 15.39 ± 7.91 % initial dose/g tissue; $P = .03$; Fig 2C). Importantly, when anatomically comparable PET sections and Masson trichrome–stained slices were examined, similar myocardial distribution patterns of radioactivity and histologically validated interstitial collagen deposits were observed (Fig 2D).

Kinetics and Specificity of T-peptide-MeCOSar Binding to Fibrotic Hearts

The kinetics and specificity of ^{64}Cu-T-peptide-MeCOSar binding to its target were then determined by PET in 9-month-old

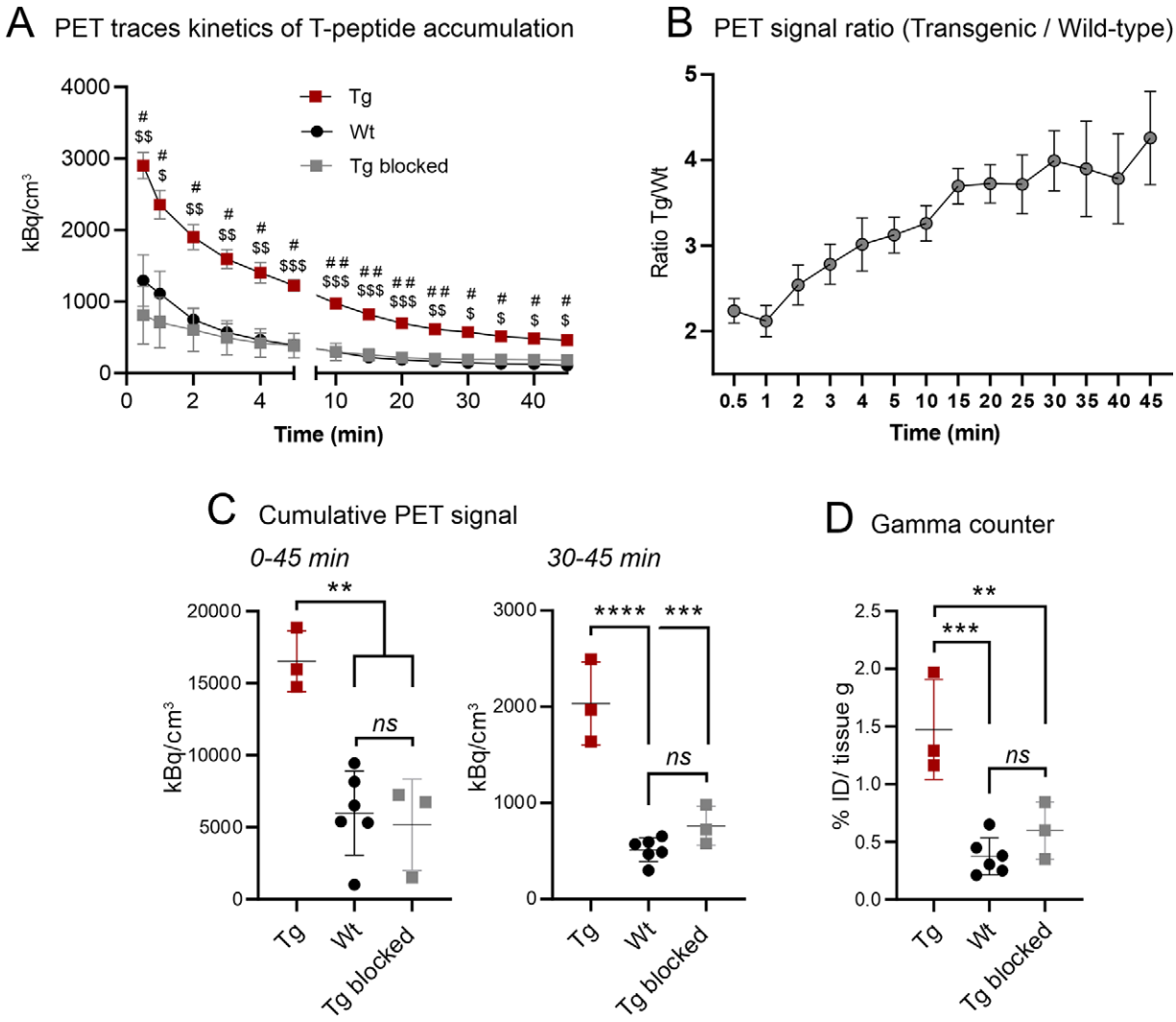

Figure 3: PET demonstration of the kinetics and blocking of cardiac copper 64 (^{64}Cu)-T-peptide-MeCOSar (chemical name, 5-(8-methyl-3,6,10,13,16,19-hexaaza-bicyclo[6.6.6]icosan-1-ylamino)-5-oxopentanoic acid) accumulation in aged fibrotic hearts. **(A)** Graph shows collated PET traces of cardiac probe accumulation over time following intravenous injection of ^{64}Cu-T-peptide-MeCOSar (0.25 mg/kg;18 MBq ± 2.7 [SD]) to aged (~9 months) β2-adrenergic receptor transgenic mice (Tg) and their nontransgenic littermate controls (Wt) or to Tg mice coadministered a 10-fold excess of non-labeled probe ("Tg blocked"). Significantly higher PET signal intensity is obtained in fibrotic Tg hearts throughout the 45-minute acquisition relative to controls while the excess nonlabeled ("cold") probe completely blocks this enhanced uptake. $^{\$, \#}$ = $q < .05$, $^{\$\$, \#\#}$ = $q < .01$, and $^{\$\$\$}$ = $q < .001$ comparing Tg versus Wt ($) or Tg versus Tg blocked (#) by repeated-measures two-way analysis of variance and post hoc corrected for multiple comparisons by controlling for the false discovery rate with the method of Benjamini, Krieger, and Yekutieli. **(B)** Graph of PET traces analysis (Tg relative to Wt in each time point in **[A]**) shows an improved signal-to-background ratio over time. The optimal window for imaging is greater than or equal to 30 minutes following tracer administration. **(C)** Graph shows quantification of the cumulative cardiac PET signal intensity obtained in vivo during the complete 45-minute recording period (left) or between 30 and 45 minutes (right) after the blood tracer pool has largely been cleared. **(D)** Graph of gamma-counter analysis of excised postmortem hearts confirms the kinetic observations. Importantly, the full inhibition of ^{64}Cu-T-peptide-MeCOSar binding by an excess cold probe is apparent. In **(C)** and **(D)**, ** = $P < .01$, *** = $P < .001$, and **** = $P < 0001$ by one-way analysis of variance with Tukey post hoc test. Data are means ± standard error of the means **(A)** or ± SDs **(B–D)**. There was a sample size of three in the Tg and Tg blocked groups and six in the Wt group. ID = initial dose, min = minutes, ns = not significant.

β2-AR Tg mice and their nontransgenic littermate controls (Fig 3). A simple main effect analysis by repeated-measures two-way one-way analysis of variance revealed that both the genotype (F = 16.65; $P < .001$) and time (F = 32.41; $P < .001$) had a statistically significant effect on the average peptide uptake over time, with a significant interaction between these terms (F = 3.713; $P < .001$). Time-activity curves demonstrated a rapid accumulation of ^{64}Cu-T-peptide-MeCOSar in the fibrotic hearts of Tg animals at 30 seconds following intravenous administration, gradually clearing over the ensuing 45 minutes (Fig 3A). Activity was significantly higher in Tg animals when compared with Wt controls across the entire acquisition period (Fig 3A; $P \leq .03$ at all time points). Coadministration of nonradioactive peptide and radiolabeled material at a 10:1 ratio in Tg mice ("Tg blocked") fully blocked T-peptide binding in the heart and reduced its levels to those seen in nontransgenic controls ($P \geq .09$ at all time points comparing Tg blocked vs Wt; $P \leq .04$ at all time points comparing Tg blocked vs Tg; Fig 3A). These results indicate a specific T-peptide uptake by the fibrotic cardiac substrate rather than representation of an increased ex-

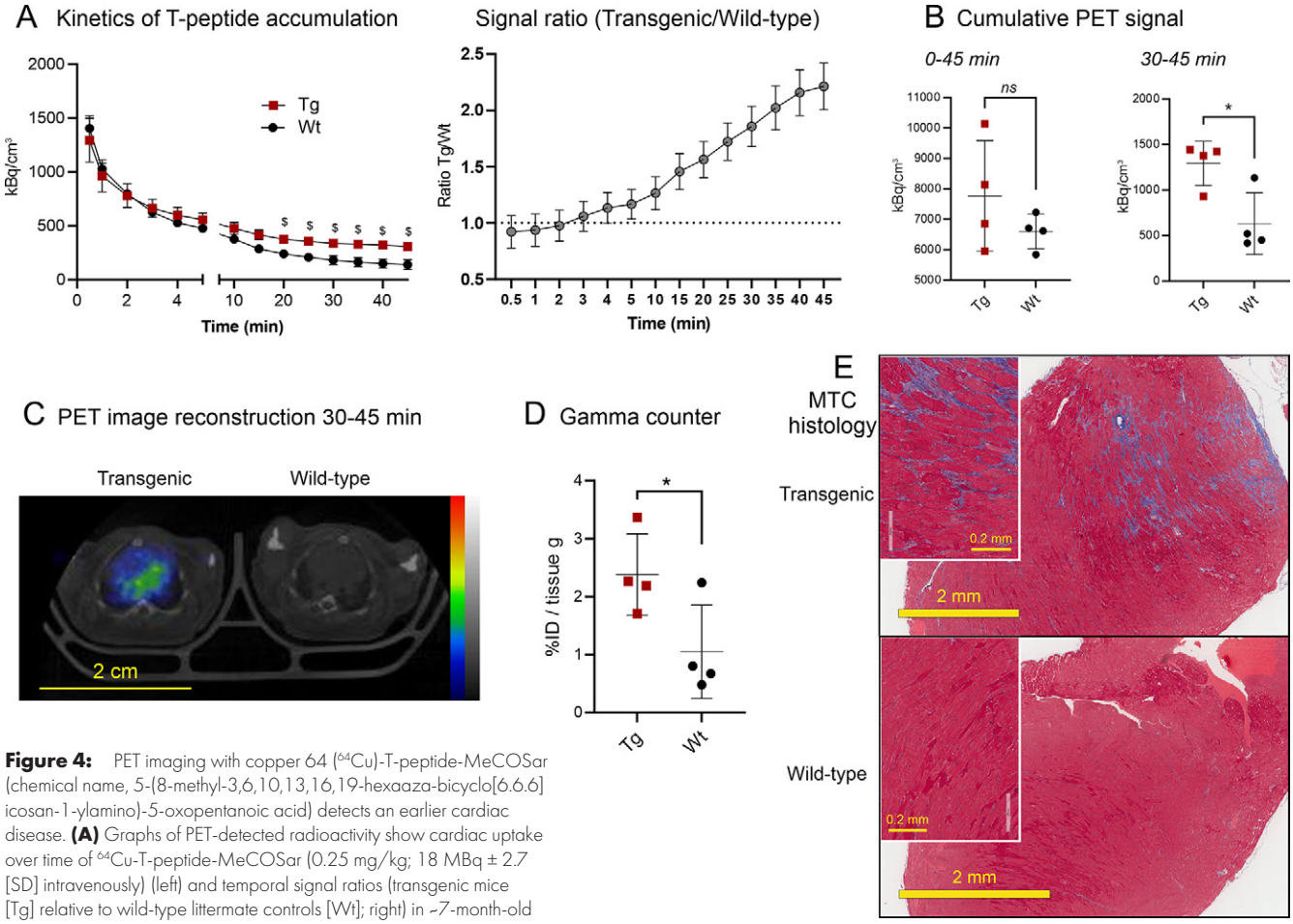

Figure 4: PET imaging with copper 64 (^{64}Cu)-T-peptide-MeCOSar (chemical name, 5-(8-methyl-3,6,10,13,16,19-hexaaza-bicyclo[6.6.6] icosan-1-ylamino)-5-oxopentanoic acid) detects an earlier cardiac disease. **(A)** Graphs of PET-detected radioactivity show cardiac uptake over time of ^{64}Cu-T-peptide-MeCOSar (0.25 mg/kg; 18 MBq ± 2.7 [SD] intravenously) (left) and temporal signal ratios (transgenic mice [Tg] relative to wild-type littermate controls [Wt]; right) in ~7-month-old β2-adrenergic receptor Tg mice with intermediate cardiac fibrosis. Optimal time-windows for imaging emerge later in the acquisition. $ = $P < .05$ comparing Tg versus Wt by repeated-measures two-way analysis of variance with uncorrected Fisher least significance difference post hoc test. **(B)** Graph shows quantification of the cumulative cardiac PET signal intensity obtained in vivo during the full 45-minute recording period (left) or between 30 to 45 minutes (right). **(C)** A representative transverse PET image reconstructed between 30 to 45 minutes following tracer injection clearly demonstrates intermediate cardiac fibrosis in a 7-month-old Tg mouse relative to Wt. **(D)** Gamma counts of excised postmortem hearts confirm the enhanced uptake of the T-peptide tracer in Tg mice as seen from the dynamic scans. In **(B)** and **(D)**, * = $P < .05$ by two-tailed Student *t* test. **(E)** Masson trichrome (MTC) histologic image of coronal heart slices show an intermediate cardiac fibrosis forming around the base of the heart in mice at 7 months of age. Data are means ± standard error of the means **(A)** or ± SDs **(B, D)**. There was a sample size of four per group. Scale bars as specified. Color scale represents PET radiotracer uptake with red corresponding to the highest activity and blue to the lowest activity. ID = initial dose, min = minutes, ns = not significant.

tracellular volume. From an imaging point of view, the ratio of fibrosis-specific (Tg) to background (Wt) PET-detected radioactivity increased over time (from 2.24-fold at 30 seconds to 4–4.26-fold at 30–45 minutes), indicating that delayed acquisition beyond 30 minutes following tracer administration represents the optimal imaging time-window (Fig 3B). Quantification of the PET radioactivity over the full (0–45 minutes) and delayed (30–45 minutes) acquisition periods (Fig 3C) and ex vivo gamma counting at 45 minutes following peptide administration (Fig 3D) confirmed both the enhanced T-peptide binding to Tg mouse hearts and the out-competition of binding by the nonlabeled probe (Fig 3C, 3D; $P \leq .007$). Of note, the PET activity data spread in the control group tightened and significance levels improved relative to the Tg group when data were collated from 30 to 45 minutes (Fig 3C; $P < .001$). This outcome is likely attributed to the improved differentiation of actual tissue binding (also indicated by higher signal ratios; Fig 3B), given that the influence of the blood pool diminishes considerably by this point. Similar results were encouragingly obtained when tracer levels were reduced 10-fold (ie, 25 μg/kg; not shown), laying foundations for a microdosing protocol adjustment of this methodology.

T-peptide–based PET Findings Can Detect Moderate Cardiac Fibrosis Associated with Early Disease

Since our initial PET scans were performed in 9–10.5-month-old β2-AR Tg mice, corresponding with severe cardiac fibrosis (10–12) (Fig 2D), we finally sought to test whether our T-peptide–based PET approach was sensitive enough to detect a more moderate cardiac disease. For this purpose, we conducted dynamic PET scans on younger animals (6.5–7.5 months old), displaying intermediate levels of heart fibrosis (10–12) (Fig 4). Simple main effect analysis by two-way repeated measures one-way analysis of variance of the entire 45 minutes showed that time ($F = 83.22$; $P < .001$), but not genotype ($F = 1.510$; $P = .27$), had a statistically significant effect on tracer uptake (Fig 4A, left). Nevertheless, a subtle enhancement of tracer uptake in the younger Tg mouse hearts could be observed from 4

minutes following tracer administration, becoming significant between 20 to 45 minutes ($P \leq .046$; Fig 4A, left). Accordingly, the ratio of measured radioactivity between diseased and healthy hearts climbed steadily from 4 minutes, reaching 2.2-fold at 45 minutes (Fig 4A, right). This profile of tracer accumulation indicated that a delayed imaging time-window may be crucial for detection of intermediate heart fibrosis. Indeed, in contrast to the pattern observed with severe cardiac fibrosis (Fig 3C), the cumulative PET radioactivity in the mildly affected hearts was not significantly different between genotypes when collated over the entire 45-minute scan (Fig 4B, left). However, when considering activity only between 30 and 45 minutes following injection, a significant difference was observed between the two genotypes (Wt: 631.0 kBq/cm^3 ± 338.4 vs Tg: 1293 kBq/cm^3 ± 243.3; 2.05-fold; $P = .02$; Fig 4B, right) which yielded a qualitatively distinct PET image (Fig 4C). Ex vivo gamma counting at the end point 45 minutes following tracer delivery confirmed a significantly higher tracer accumulation in younger Tg hearts relative to Wt controls (Wt: 1.05 ± 0.81 vs Tg: 2.38 ± 0.7 % initial dose/g tissue; 2.27-fold; $P = .047$; Fig 4D). Notably, Masson trichrome histologic analysis revealed the presence of diffuse cardiac fibrosis in younger animals mainly toward the base of heart (Fig 4E) but not throughout the myocardium as previously observed in older animals (Fig 2D).

Discussion

This work demonstrated in a mouse model of heart disease the value of T-peptide–based PET imaging as a noninvasive technique for assessment of diffuse cardiac fibrosis, representing a potential breakthrough in molecular imaging of this serious and common heart pathology. Specifically, our data underpinned the collagen-targeting nature of the T-peptide and indicated its capacity to enrich fibrotic heart tissue in a rapid and specific manner, enabling in vivo imaging of interstitial cardiac fibrosis at various degrees of severity to demonstrate the underlying cardiomyopathy. Furthermore, we established that delayed acquisition protocol (between 30 and 45 minutes following tracer administration) was desirable for PET imaging of intermediate cardiac fibrosis that is associated with an earlier heart disease.

Several targeted probes have been described for molecular imaging of cardiac disease (15), yet limitations still exist and not all clinical challenges have been addressed. The collagen I–targeting peptide EP-3533, for example, enhanced myocardial scars at cardiac MRI in murine models of myocardial infarction (7,8) but was never evaluated against diffuse interstitial fibrosis. More recently, PET imaging using a gallium 68–labeled fibroblast activation protein inhibitor tracer could demonstrate myocardial infarction (16) and possibly early stages of HF (17) by exploitation of fibroblast activation protein expression on activated cardiac fibroblasts. While seemingly promising for early detection of active myocardial fibrosis, gallium 68–labeled fibroblast activation protein inhibitor uptake peaks early in the HF process (17) and may be less suitable for monitoring disease progression over time or regression during therapeutic interventions. Our PET approach for direct imaging of MMP-digested cardiac collagen IV using the ^{64}Cu-T-peptide-MeCOSar could provide a unique tool for long-term monitoring of progression and/or its response to treatment both in the early and advanced stages to enable improved patient stratification and therapy assessment. Moreover, being directed against a substrate that is often present in many cardiomyopathies, T-peptide applications could be extended for theranostic purposes and direction of medications into the heart.

Despite the advantages of collagen targeting over time, it is a requisite for a cardiac molecular probe to detect active heart pathology early with high sensitivity and facilitate effective and timely intervention (15). Encouragingly, our current results were obtained in both severely fibrotic hearts of aged β2-AR mice (9–10.5 months old) (10–12,14) and younger mice (~7 months old) displaying intermediate cardiac disease. Given the over twofold difference in the cumulative cardiac radioactivity strength between Tg and control mice even in younger animals, we believe that this PET approach is likely to distinguish a much earlier cardiac disease and provide opportunity for early intervention. Assessment of the limits in temporal sensitivity of the T-peptide probe, however, requires further examination.

Another question of interest is whether T-peptide–based imaging can be harnessed to monitor and characterize cardiac fibrosis in a wide range of heart diseases, such as the cardiac scarring inflicted by myocardial infarction. This capability may not be trivial due to core differences that exist between the processes underlying chronic cardiac fibrosis and the dynamic nature of scar formation following myocardial infarction. Most importantly, although cardiac tissue undergoing HF-dilated cardiomyopathy and hypertrophic cardiomyopathy contains collagen IV in both basement membrane–related fibrotic lesions and in patches of replacement fibrosis (1,4,18) (as we have also shown in the β2-AR model [4]), the main collagen types upregulated in regions of myocardial infarction are fibrillar extracellular matrix collagens, like types I and III (19). Yet, the strong angiogenic response that begins in the infarct border zone (20), as well as emerging strategies to enhance angiogenesis following myocardial infarction and preserve cardiomyocytes (together with their basement membrane) (21), might provide sufficient levels of collagen IV–containing substrate for T-peptide–based imaging to succeed. One could further speculate that imaging with the T-peptide could enable evaluation of the degree of neovascularisation and cardiomyocyte preservations following myocardial infarction, predicting the long-term damage, potential for repair, and directing suitable interventions to minimize progression into HF. Other adjustments for the use of T-peptide–based imaging may be required due to changes in the expression and distribution patterns of collagen IV and MMPs in different heart conditions. For example, collagen IV is reported by some to be restricted to the myocyte basement membrane in hypertrophic cardiomyopathy but present in fibrotic lesions throughout the myocardium in dilated myocardial hypertrophy (18), possibly affecting the signal strength and interpretation of the PET scan. These important considerations remain to be investigated in a broader range of cardiac pathology models.

Since only male mice were used in this study, it will be essential to assess the suitability of the T-peptide approach also in female mice. Along with the known lower rates of

cardiovascular disease morbidity and mortality in female individuals (22,23), it is also reported that cardiac fibrosis and heart inflammation is generally less severe during disease and/or aging in female individuals relative to male individuals (23,24). Despite an eventual build-up of collagen in the hearts of both male and female patients during pathology, and even though digested collagen IV (the T-peptide's substrate) by itself is not specific to sex, the total collagen amounts and distribution patterns, as well as cardiac inflammation and MMP-mediated collagen turnover processes, substantially differ in the hearts of female as compared with male patients (23–25). As such, sex-specific fibrotic changes in the female heart may affect image characteristics, sensitivity, and interpretation of a T-peptide–based PET scan. While it stands to reason that the probe can also be used efficiently in female individuals once cardiac fibrosis has developed, purposely designed preclinical experiments that encompass female mice are required to assess this important matter.

From a translational point of view, a rapid pathway for translation and clinical implementation of this approach is feasible considering *(a)* the human collagen IV specificity of the T-peptide (6), *(b)* our earlier ex vivo proof-of-concept results which demonstrated uptake in clinical heart specimens (4), and *(c)* the successful use of the MeCOSar chelator in clinical trials for other indications (eg, cancer diagnosis [26] or imaging of HIV [27]). Furthermore, a few lines of evidence point to superior safety and toxicity profiles of the T-peptide radiotracer, including *(a)* a lack of known biologic activities of this tracer beside binding to MMP-2–digested collagen IV (indeed, we reported the probe to be nontoxic to hepatic and renal tissue and well tolerated by mice [4]); *(b)* the short half-life of ~9 minutes (4) and biodegradable nature of the tracer, which would translate into fast clearance and reduced long-term tissue accumulation, respectively; *(c)* our radio-HPLC data indicating no free ^{64}Cu after labeling; and *(d)* our promising imaging studies reported here with a 10-fold less peptide amount (ie, 25 μg/kg instead of 250 μg/kg), which all increase our confidence in the safety of this methodology.

While we do not anticipate the T-peptide radiotracer to cause any substantial toxic adverse effects with clinical use, the radiation exposure to patients and the logistical issues associated with radioactive imaging agents will need to be considered when assessing the clinical viability of this new approach when compared with other imaging modalities. PET imaging is becoming a viable routine diagnostic test for treatment guidance in various cancers and beyond, and several ^{64}Cu-based imaging agents are currently being evaluated in humans (26–28). The translation of this new tracer to the clinic will require assessment of radiation dosimetry to nontarget organs.

In summary, the substantial involvement of collagen IV–containing interstitial cardiac fibrosis in many heart conditions, as well as the quantitative and qualitative sensitivity of PET, implies that the T-peptide tracer could have broad applicability in cardiology as a unique molecular imaging probe for visualization of diffuse cardiac fibrosis. The capacity to distinguish the state of the heart in a simple and noninvasive way could enable disease stratification, long-term monitoring, and much-needed guidance of optimal treatment choices.

Acknowledgments: The authors acknowledge the facilities, as well as scientific and technical assistance of the National Imaging Facility (NIF), a National Collaborative Research Infrastructure Strategy (NCRIS) capability at Monash Biomedical Imaging (MBI; Monash University). We further thank the Histology Platform of Monash University for their professional support and the dedicated staff of the Precinct Animal Centre (PAC) for their assistance and colony care during this project. The authors wish to express their gratitude to the donors of the Heart Foundation of Australia for the kind generosity. Finally, the authors express gratitude to the Community and Engagement program at the Centre Clinical School, Monash University for their invaluable assistance in connecting with a community member who contributed their lived experience and actively participated in this project.

Author contributions: Guarantors of integrity of entire study, **B.N.**, **R.X.**, **K.A.**; study concepts/study design or data acquisition or data analysis/interpretation, all authors; manuscript drafting or manuscript revision for important intellectual content, all authors; approval of final version of submitted manuscript, all authors; agrees to ensure any questions related to the work are appropriately resolved, all authors; literature research, **B.N.**, **R.X.**, **M.E.**, **C.E.H.**, **K.A.**; experimental studies, all authors; statistical analysis, **B.N.**, **B.J.**, **C.E.H.**, **K.A.**; and manuscript editing, **B.N.**, **B.J.**, **R.X.**, **P.S.D.**, **C.E.H.**, **K.A.**

Disclosures of conflicts of interest: **B.N.** No relevant relationships. **B.J.** No relevant relationships. **N.A.Z.** Employed as a research assistant by P.S.D. at the University of Melbourne. **R.X.** No relevant relationships. **E.J.** No relevant relationships. **M.E.** No relevant relationships. **A.N.** No relevant relationships. **P.S.D.** Listed as an inventor on intellectual property that relates to the MeCOSar chelator that has been assigned to Clarity Pharmaceuticals from the University of Melbourne; shareholder in Clarity Pharmaceuticals; serves on the scientific advisory board for Clarity Pharmaceuticals. **C.E.H.** No relevant relationships. **K.A.** No relevant relationships.

References

1. Nogami K, Kusachi S, Nunoyama H, et al. Extracellular matrix components in dilated cardiomyopathy. Immunohistochemical study of endomyocardial biopsy specimens. Jpn Heart J 1996;37(4):483–494.
2. Wang GY, Bergman MR, Nguyen AP, et al. Cardiac transgenic matrix metalloproteinase-2 expression directly induces impaired contractility. Cardiovasc Res 2006;69(3):688–696.
3. Stirrat J, White JA. The prognostic role of late gadolinium enhancement magnetic resonance imaging in patients with cardiomyopathy. Can J Cardiol 2013;29(3):329–336.
4. Ezeani M, Noor A, Alt K, et al. Collagen-Targeted Peptides for Molecular Imaging of Diffuse Cardiac Fibrosis. J Am Heart Assoc 2021;10(18):e022139.
5. Ezeani M, Noor A, Donnelly PS, Niego B, Hagemeyer CE. Assessment of the epi-pericardial fibrotic substrate by collagen-targeted probes. Sci Rep 2022;12(1):5702.
6. Mueller J, Gaertner FC, Blechert B, Janssen KP, Essler M. Targeting of tumor blood vessels: a phage-displayed tumor-homing peptide specifically binds to matrix metalloproteinase-2-processed collagen IV and blocks angiogenesis in vivo. Mol Cancer Res 2009;7(7):1078–1085.
7. Caravan P, Das B, Dumas S, et al. Collagen-targeted MRI contrast agent for molecular imaging of fibrosis. Angew Chem Int Ed Engl 2007;46(43):8171–8173.
8. Helm PA, Caravan P, French BA, et al. Postinfarction myocardial scarring in mice: molecular MR imaging with use of a collagen-targeting contrast agent. Radiology 2008;247(3):788–796.
9. Paterson BM, Roselt P, Denoyer D, et al. PET imaging of tumours with a 64Cu labeled macrobicyclic cage amine ligand tethered to Tyr3-octreotate. Dalton Trans 2014;43(3):1386–1396.
10. Du X-J, Autelitano DJ, Dilley RJ, Wang B, Dart AM, Woodcock EA. β(2)-adrenergic receptor overexpression exacerbates development of heart failure after aortic stenosis. Circulation 2000;101(1):71–77.
11. Nguyen MN, Kiriazis H, Ruggiero D, et al. Spontaneous ventricular tachyarrhythmias in β2-adrenoceptor transgenic mice in relation to cardiac interstitial fibrosis. Am J Physiol Heart Circ Physiol 2015;309(5):H946–H957.
12. Xu Q, Dalic A, Fang L, et al. Myocardial oxidative stress contributes to transgenic β_2-adrenoceptor activation-induced cardiomyopathy and heart failure. Br J Pharmacol 2011;162(5):1012–1028.
13. Alt K, Paterson BM, Ardipradja K, et al. Single-chain antibody conjugated to a cage amine chelator and labeled with positron-emitting copper-64 for diagnostic imaging of activated platelets. Mol Pharm 2014;11(8):2855–2863.
14. Nguyen MN, Su Y, Kiriazis H, et al. Upregulated galectin-3 is not a critical disease mediator of cardiomyopathy induced by β_2-adrenoceptor overexpression. Am J Physiol Heart Circ Physiol 2018;314(6):H1169–H1178.

15. Ezeani M, Hagemeyer CE, Lal S, Niego B. Molecular imaging of atrial myopathy: Towards early AF detection and non-invasive disease management. Trends Cardiovasc Med 2022;32(1):20–31.
16. Yuan T, Wang X. ^{68}Ga-FAPI PET/MRI in Coronary Heart Disease. J Nucl Cardiol 2022;29(6):3608–3610.
17. Song W, Zhang X, He S, et al. ^{68}Ga-FAPI PET visualize heart failure: from mechanism to clinic. Eur J Nucl Med Mol Imaging 2023;50(2):475–485.
18. Watanabe T, Kusachi S, Yamanishi A, et al. Localization of type IV collagen alpha chain in the myocardium of dilated and hypertrophic cardiomyopathy. Jpn Heart J 1998;39(6):753–762.
19. Schumacher D, Curaj A, Staudt M, et al. Endogenous Modulation of Extracellular Matrix Collagen during Scar Formation after Myocardial Infarction. Int J Mol Sci 2022;23(23):14571.
20. Wu X, Reboll MR, Korf-Klingebiel M, Wollert KC. Angiogenesis after acute myocardial infarction. Cardiovasc Res 2021;117(5):1257–1273.
21. Li J, Zhao Y, Zhu W. Targeting angiogenesis in myocardial infarction: Novel therapeutics (Review). Exp Ther Med 2022;23(1):64.
22. Bots SH, Peters SAE, Woodward M. Sex differences in coronary heart disease and stroke mortality: a global assessment of the effect of ageing between 1980 and 2010. BMJ Glob Health 2017;2(2):e000298.
23. Kessler EL, Rivaud MR, Vos MA, van Veen TAB. Sex-specific influence on cardiac structural remodeling and therapy in cardiovascular disease. Biol Sex Differ 2019;10(1):7.
24. Lau ES, Kaur G, Sharma G. Sex and Age Differences in Myocardial Fibrosis. JACC Adv 2023;2(3):100332.
25. Chehab O, Shabani M, Varadarajan V, et al. Endogenous Sex Hormone Levels and Myocardial Fibrosis in Men and Postmenopausal Women. JACC Adv 2023;2(3):100320.
26. Hicks RJ, Jackson P, Kong G, et al. ^{64}Cu-SARTATE PET Imaging of Patients with Neuroendocrine Tumors Demonstrates High Tumor Uptake and Retention, Potentially Allowing Prospective Dosimetry for Peptide Receptor Radionuclide Therapy. J Nucl Med 2019;60(6):777–785.
27. McMahon JH, Zerbato JM, Lau JSY, et al. A clinical trial of non-invasive imaging with an anti-HIV antibody labelled with copper-64 in people living with HIV and uninfected controls. EBioMedicine 2021;65:103252.
28. Carlsen EA, Johnbeck CB, Loft M, et al. Semiautomatic Tumor Delineation for Evaluation of ^{64}Cu-DOTATATE PET/CT in Patients with Neuroendocrine Neoplasms: Prognostication Based on Lowest Lesion Uptake and Total Tumor Volume. J Nucl Med 2021;62(11):1564–1570.